Astron. Astrophys. 320, 228–236 (1997)

ASTRONOMY AND ASTROPHYSICS

Fundamental parameters of Cepheids

IV. Radii and luminosities

D. Bersier[1], **G. Burki**[1], **and R.L. Kurucz**[2]

[1] Observatoire de Genève, 51 ch. des Maillettes, CH-1290 Sauverny, Switzerland
[2] Harvard-Smithsonian Center for Astrophysics, 60 Garden Street, Cambridge, MA 02138, USA

Received 3 July 1996 / Accepted 25 September 1996

Abstract. A temperature scale for Cepheids is presented, based on Geneva photometry. It uses new atmosphere models computed at various values of microturbulent velocity. The scale so-obtained is compared to other ones and the importance of microturbulence effects is shown.

This calibration is applied to 20 Cepheids for which the variation of microturbulence is known. The detailed variations of temperature and gravity are derived. The behavior of the photometric gravity is in very good agreement with the effective gravity (sum of GM/R^2 and of the derivative of the radial velocity). Thus static atmosphere models can be used to describe the temperature and gravity variations in Cepheids under the following conditions: *i)* the microturbulence has to be taken into account, *ii)* the effective gravity must be considered instead of the static gravity, *iii)* in some cases, a small phase interval around minimum radius does not give reliable results.

The temperature and bolometric corrections are then used to derive radii and distances via the Baade-Wesselink technique. The resulting Period-Radius and Period-Luminosity relations are discussed. Our results compare very well with similar analysis based on infra-red (JHK) photometry.

Key words: stars: atmospheres – stars: fundamental parameters – stars: late-type – Cepheids

1. Introduction

The final goal of this series of papers is to apply a revised version of the Baade-Wesselink method (that allows to determine the mean radius of a pulsating star) to a sample of Cepheids, well measured in Geneva photometry and radial velocity (Bersier et al. 1994a, 1994b, hereafter papers I and II). Recall that this method, in its simplest variants, requires a one-to-one relation between a colour index and the effective temperature. However, everybody is aware that the colours used in BW analyses can suffer from "contamination" by gravity and microturbulence. While it seems that e.g. $V-R$ is not sensitive to gravity (Barnes & Evans 1976), almost no attempt has been made to quantify the effect of the variation of microturbulent velocity on the colours. In this paper we will directly derive the temperatures and bolometric corrections from atmosphere models computed at different values of microturbulent velocity. The second aim will be to apply the Baade-Wesselink method with the temperatures and bolometric corrections so derived.

The Geneva photometric system, with its high internal accuracy and homogeneity, is suited to the study of a variety of astrophysical problems. The calibrations that have appeared in the last years cover a large fraction of the HR diagram (North & Nicolet 1990, Kobi & North 1990, Künzli et al. 1996). In most cases however, the samples of comparison stars contain mostly dwarfs and subgiants. This means that these calibrations are not applicable to cool supergiant stars, so we cannot use previous work in Geneva photometry for our present purpose. Fundamental parameters ($T_{\rm eff}$, $\log g$ and BC) will be determined by combining observed colours and synthetic fluxes. Thanks to recent models, microturbulence can be taken into account. These parameters are used in conjunction with radial velocity measurements (Bersier et al. 1994b) to derive absolute magnitudes and radii.

The paper is organized as follows: in Sect. 2 are described the models and the synthetic colours. The resulting gravities and temperatures for Cepheids are discussed in Sect. 3. The Baade-Wesselink method is applied in Sect. 4 where we give the radii and luminosities. Then follows a discussion of the Period-Radius and Period-Luminosity relations.

2. Atmosphere models and synthetic colours

2.1. Atmosphere models

With the advent of a new generation of computers, it has become possible to make much more accurate opacity calculations by taking into account a very large number of lines. In the current Kurucz models, no less than 58 million atomic and molecular

Send offprint requests to: D. Bersier

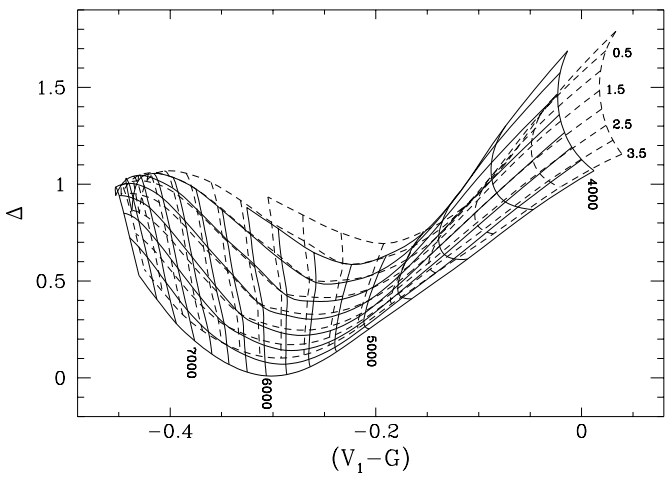

Fig. 1. In order to see the effects of microturbulence on the colours, two grids are superimposed in this figure, at ξ_t = 2 km s^{-1} (solid lines) and ξ_t = 4 km s^{-1} (dashed lines). The temperature ranges from 4000 K to 7750 K (step=250 K), the gravity from 0 to 3.5 (step=0.5 dex). One can see that, for a given pair of values ($V_1 - G$, Δ), the temperature will be larger if the microturbulence is increased, since the whole grid is displaced to the right. The effect on the gravity depends on the exact position on the grid; for temperatures above $\sim$ 5000 K, $\log g$ will be larger

lines are incorporated. In the last few years, new opacity distribution functions have been computed, for metallicities ranging from [-5.0] to [+1.0] and at five different values of microturbulent velocity: 0, 1, 2, 4, 8 km s^{-1} (Kurucz 1991, 1992). These are distributed on Kurucz CD-ROMs 2-12 and 14.

A grid of models has been computed by one of us (RLK) for all these metallicities (at ξ_t = 2 km s^{-1}) supplemented by models at solar metallicity and for all the five microturbulent velocities. For all these models, fluxes have been computed with a resolution of 2 nm in the visible which is adequate for synthetic photometry (Kurucz 1993, 1994).

Since then, a conceptual error has been detected in the ATLAS9 code by Castelli (1994, see also 1996). An inconsistency occurred when the convective flux is zero at the last depth in the model because the convection zone is wholly contained in the atmosphere. The program computed convection differently depending on whether the last value was zero or not. The program has now been changed to be consistent and now color-color diagrams are more regular in the weakly convective region. The new convective models and fluxes will be available on CD-ROMs (Kurucz 1996).

In the present study, we will only use the new models that cover a small part of the complete grids. The temperature range is 4000-7500 K, the gravity range is 0.0-3.5, for each of the five values of microturbulent velocity given above, at solar metallicity. This grid is a three-dimensional space where the axes are $T_{\rm eff}$, $\log g$ and ξ_t.

2.2. Synthetic colours

Synthetic photometry is only the simulation of the observation process. The accuracy with which the passbands of the considered system are known is important, since this determines the discussion of possible differences between observed and synthetic colours. In Geneva photometry, the passbands are well known (Rufener & Nicolet 1988) so this exercise is possible. For each flux of the grid, synthetic magnitudes have been computed in the seven passbands of the Geneva photometric system and relevant colour indices have been formed. We decided to work with subgrids defined by $V_1 - G$ and Δ. An example of such a subgrid is given in Fig. 1.

The reddening-free parameter Δ is a good gravity indicator for cool stars (see e.g. Golay 1980). It is defined as

$$\Delta = (U - B_2) - 0.832(B_2 - G). \quad (1)$$

The colour index $V_1 - G$ is mostly a temperature indicator, as can be seen on Fig. 1. With $V_1 - G$ and Δ, one can separate the effects of gravity and temperature. They are also sensitive to microturbulence variations, thus the choice of these parameters appeared natural.

3. Temperature and gravity for Cepheids

The essential ingredient of our version of the BW method is the inclusion of microturbulence. The microturbulent velocity ξ_t as a function of phase has been determined for each Cepheid in Paper III. We will recall the most important steps leading to this determination. Our radial velocity measurements have been obtained with the use of the cross-correlation technique. We showed in paper III that a fraction of the width of the cross-correlation function is related to turbulence and this relation has been quantified. By fitting a Fourier series to what we have called the *residual width*, we thus have a value of the microturbulent velocity at each phase.

3.1. Temperature

For each photometric observation of a given Cepheid, we can extract $T_{\rm eff}$ and $\log g$ from the grids of synthetic colours. The colour excess for each star has been computed following the method exposed in Bersier (1996). We enter in each subgrid at constant $\xi_t$with $(V_1 - G)_0$ and Δ. By two-dimensional interpolation, we obtain a temperature and a gravity. Since there are five subgrids (at 0, 1, 2, 4 and 8 km s^{-1}), we have five $T_{\rm eff}$ and $\log g$. It is then simple to interpolate between these five values of $T_{\rm eff}$ (respectively $\log g$) as a function of ξ_t for obtaining the temperature (respectively gravity) corresponding to the observed microturbulent velocity. One also obtains the bolometric correction. For each Cepheid, we thus have $T_{\rm eff}$, $\log g$ and the bolometric correction as a function of phase. Some examples are given in Fig. 2

In Fig. 3 is shown the main result of our accounting for microturbulent velocity variations. As could be guessed from

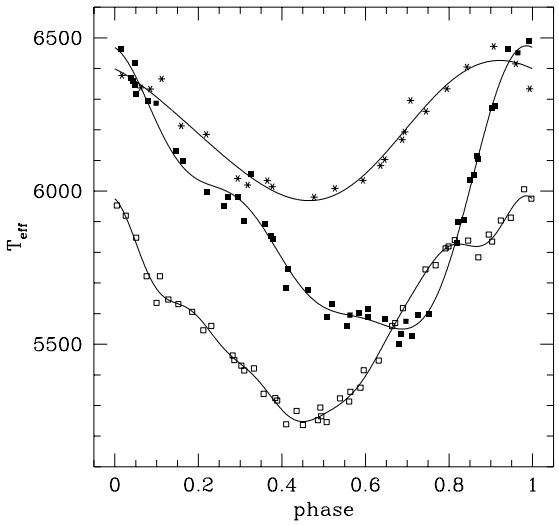

Fig. 2. Three examples of the temperature variations obtained after applying the procedure described in Sect. 2. The curves are shown for the Cepheids SZ Tau (stars), U Sgr (black squares) and S Nor (open squares), having periods of 3.15, 6.75 and 9.75 days respectively

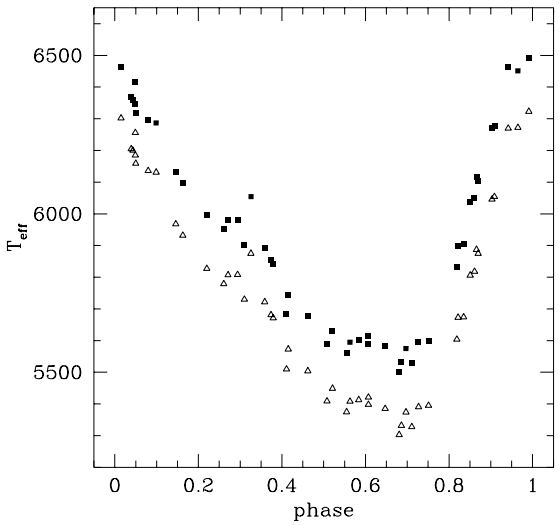

Fig. 3. The temperature curves for U Sgr obtained by using the variation of microturbulence (squares) or by keeping $\xi_{\rm t}$ at a constant value of 2 km s^{-1}(triangles). One can clearly see that with the new scale, Cepheids have larger temperatures. This is the most important effect of microturbulence

Fig. 1, the temperature is larger since the value of microturbulent velocity is larger than 2 km s^{-1}.

There is another reason why we used V_1-G and Δ. With this procedure, one needs a one-to-one relation between (V_1-G, Δ) and ($T_{\rm eff}$, $\log g$). With other parameters, like B_2-V_1 and d that have often been used in this kind of work (Künzli et al. 1996), the relation between colour indices and fundamental parameters is not unique in a certain domain of values. This means that with

Table 1. The minimum, mean and maximum temperature for the 21 Cepheids of our sample. We also give the error on the mean temperature (from a Fourier fit)

Star	$\log P$	$T_{\rm eff}$ min	$T_{\rm eff}$ mean	$T_{\rm eff}$ max	$\sigma_{\rm fit}$
V636 Cas	0.9230	5655	5765	5874	7
X Cyg	1.2145	4826	5247	5900	16
DT Cyg	0.3978	6026	6190	6378	9
BB Gem	0.3633	5765	6407	7507	49
DX Gem	0.4965	6137	6388	6639	25
ζ Gem	1.0065	5255	5501	5776	7
V473 Lyr	0.1734	6155	6286	6418	10
BE Mon	0.4322	5824	6141	6621	14
V465 Mon	0.4335	6306	6541	6882	22
V508 Mon	0.6163	5962	6240	6624	14
S Nor	0.9892	5248	5593	5984	3
V340 Nor	1.0526	5345	5555	5712	7
V440 Per	0.8792	5868	5934	6003	3
U Sgr	0.8290	5550	5926	6474	5
W Sgr	0.8805	5355	5769	6324	5
EU Tau	0.3227	6185	6404	6626	7
ST Tau	0.6058	5718	6106	6876	9
SW Tau	0.1996	5859	6363	7046	19
SZ Tau	0.4982	5969	6197	6426	7
T Vul	0.6469	5639	6008	6505	9
SV Vul	1.6532	4801	5290	6056	12

observed values of B_2-V_1 and d, one would obtain two pairs ($T_{\rm eff}$, $\log g$). V_1-G and Δ allows to alleviate this degeneracy.

3.2. Comparison with other temperature scales

Numerous attempts to determine a temperature scale applicable to Cepheids can be found in the literature. Fig. 4 shows some of them, as well as the mean temperatures derived in the present paper. A striking feature of this graph is that there is not a general agreement between the authors about the temperature scale to use for Cepheids. The present theoretical scale seems to be close to those of Pel (1985) and Johnson (1966).

It is not our aim to critically review the different temperature scales but we can say that, taking into account the variation of microturbulent velocity gives temperatures that, without any correction, are in good agreement with other scales. This shows that atmosphere models are able to reproduce fairly well empirically determined temperatures of Cepheids.

3.3. Gravity

In order to understand the physical sense of the gravity obtained with the procedure described above, we recall the definition of the effective gravity $g_{\rm eff}$ as

$$g_{\rm eff} = \frac{d^2R}{dt^2} + \frac{G\,M}{R^2} \qquad (2)$$

where d^2R/dt^2 is obtained by taking the derivative of the radial velocity curve. Figs. 5, 6 and 7 show the effective gravity and the synthetic gravity as a function of phase for our three example Cepheids. Also shown is the static gravity GM/R^2. For this comparison, a Period-Mass and a Period-Radius relations have been used (Gieren 1989, Gieren et al. 1989).

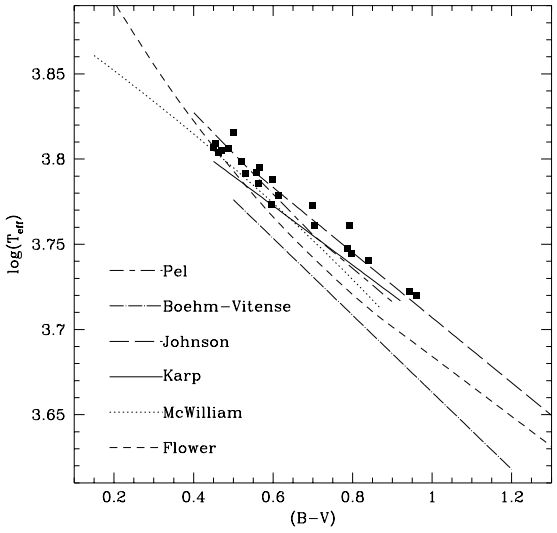

Fig. 4. This figure shows various temperature scales that appeared in the literature. They are those of Flower (1977), McWilliam (1991), Karp (1975), Johnson (1966), Böhm-Vitense (1972) and Pel (1985). Also shown are the mean value for each Cepheid in our sample (squares). The present theoretical scale is in good agreement with Pel's one at the warm temperature end and there is an overall agreement with Johnson's scale

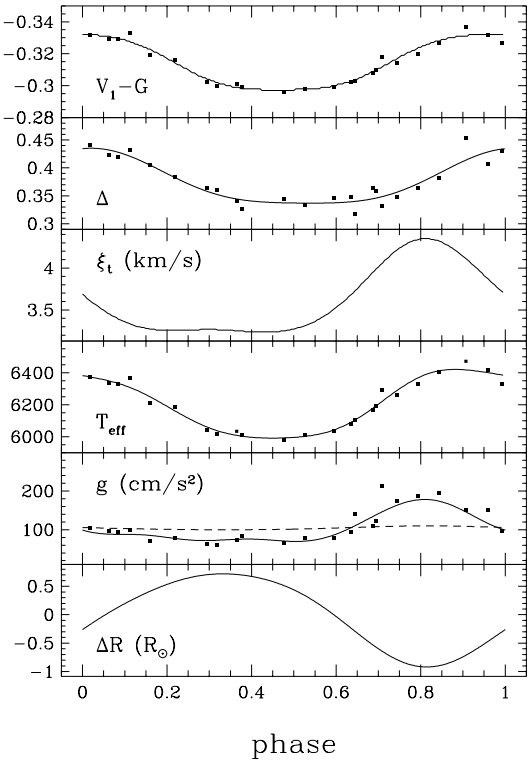

Fig. 5. This figure summarizes the steps followed to obtain $T_{\rm eff}$and $\log g$. Starting from the colours $V_1 - G$, Δ, and the microturbulent velocity $\xi_{\rm t}$, one obtains $T_{\rm eff}$ and g. The radius variation is obtained by integration of the radial velocity curve. The dashed line accompanying the gravity is GM/R^2. The solid line is the effective gravity, vertically shifted to show the resemblance between $g_{\rm eff}$ and the photometric gravity (squares). This shift corresponds to a change in mass and radius of 13%. All these curves are for the star SZ Tau

The comparison of the three kinds of gravities in Figs. 5, 6 and 7 gives us the sense of the synthetic gravity derived in this paper. One can see the striking resemblance between the shape of the $g_{\rm eff}$ curve and the synthetic gravity, particularly for U Sgr and S Nor. This appearance already tells us that the gravity measured by photometry is very close to the effective gravity, and not to the static gravity. This shows that, except around minimum radius, static atmosphere models represent very well the observed colours of Cepheids.

Apart from the excellent agreement between the shapes of the synthetic and effective gravities, there are two points that deserves further comments: the vertical shift that should be introduced for SZ Tau and the difference at minimum radius for U Sgr and S Nor. Our three examples have been chosen in order to show the major characteristics of the results. All the stars of our sample show one or several of these features at a time. There is always a good agreement on the shapes of the gravity curves; at the same time one of the discrepant points is present, or even both.

Let us discuss first the disagreement at minimum radius (like U Sgr and S Nor). The most likely cause is to be found in the presence of velocity gradients in the atmospheres of pulsating stars. A velocity gradient will broaden the spectral lines, hence the cross-correlation function (CCF). This CCF is used to derive the turbulent velocity (Bersier & Burki, 1996). Thus, at phases when there are large gradients, this velocity will be overestimated. This means that, for a given pair of colours ($V_1 - G$, Δ), the temperature and gravity derived from the procedure exposed in Sect. 2 will be different. A look at Fig. 1 shows that when $\xi_{\rm t}$ is increased, the whole grid is displaced towards the right and upward (except at low g and low $T_{\rm eff}$). This means that the computed gravity will be larger. There will also be an effect on the temperature but it will be smaller.

Concerning the vertical shift (SZ Tau), one can modify the mass and radius until agreement is reached for a phase close to ~ 0.4, that is around maximum radius, where velocity gradients will have less influence (see e.g Fokin et al., 1996). In fact, changes in M or R are usually smaller than 10% for most of the stars, and are generally smaller for the radius than for the mass. This method of determining gravity could be a new way towards the knowledge of Cepheid masses.

Another remark is related to the abundance pattern used in the models. Cepheids are evolved stars in which, for instance, C is depleted and N is enhanced (see e.g. Lambert & Ries 1981, Luck 1991). However, the models have been computed with solar abundance ratios. Tripicco & Bell (1991) showed that a change in the C and N abundances (with respect to solar values) can have non-negligible effects on the colours. Thus the next step of this procedure would be to incorporate these chemical composition changes in the models.

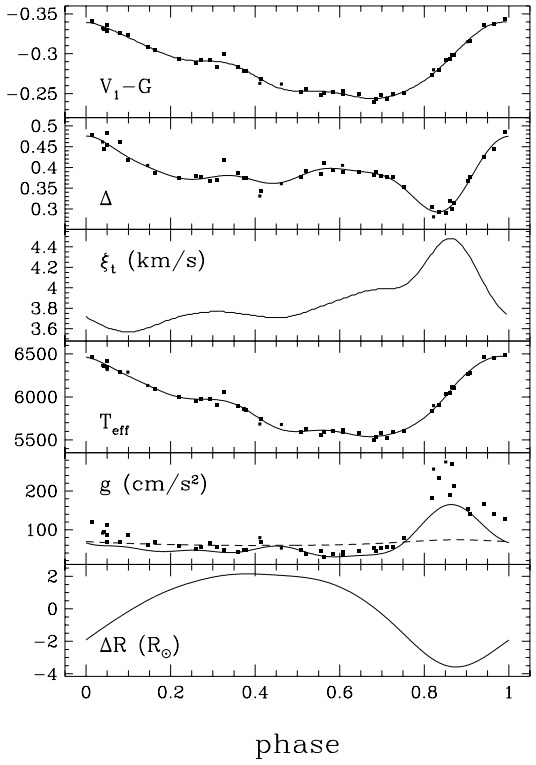

Fig. 6. Same as Fig. 5 but for U Sgr. The effective gravity has not been shifted since the agreement here is very good near maximum radius

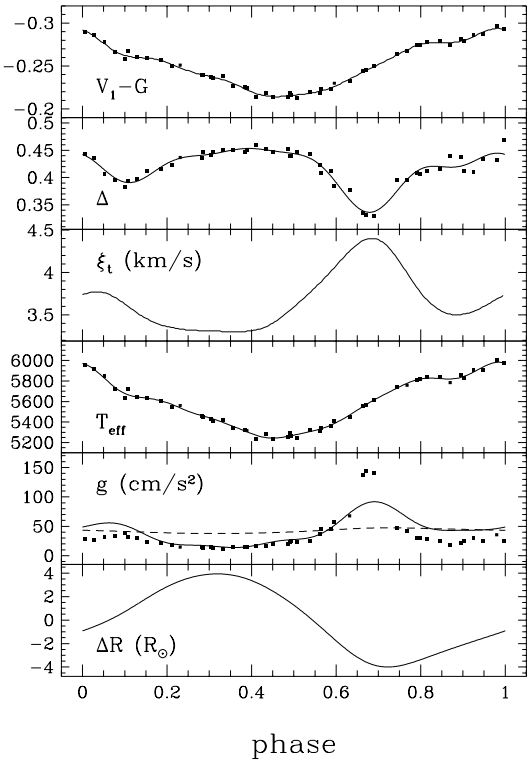

Fig. 7. Same as Fig. 5 but for S Nor. As for U Sgr, the effective gravity curve has not been shifted

4. Application of the Baade-Wesselink method

The variant of the Baade-Wesselink method that we use has already been presented in Burki & Meylan (1986), we will only give an outline of the method. Starting from the definition of the effective temperature and of the distance modulus, one can easily show that

$$\log(R/R_\odot) = -2\log T_{\rm eff} - 0.2(m_{\rm V} + BC) + \log d + 0.2A_{\rm V} + 7.472 \quad (3)$$

where BC is the bolometric correction, d is the distance to the star (in pc) and $A_{\rm V}$ is the extinction in V. By defining

$$X = \exp_{10}\{-2\log T_{\rm eff} - 0.2(m_{\rm V} + BC)\} \quad (4)$$

$$B^{-1} = \exp_{10}\{0.2A_{\rm V} + \log d + 7.472\} \quad (5)$$

$$A = R_0 B, \quad (6)$$

one has

$$X = A + B\Delta R \quad (7)$$

where $\Delta R = R - R_0$ (in solar units). ΔR is known from the integration of the radial velocity curve, A and B are determined for each star by least-squares from all photometric measurements. These parameters are constant for a given star. Knowing these, R_0 and d can easily be determined from Eqs (5) and (6). The total extinction $A_{\rm V}$ is computed from the colour excess $E(B-V)$ with $A_{\rm V} = 3.1E(B-V)$, the reddenings have been taken from Bersier (1996). The uncertainty on the individual radii are computed from the formal error on A and B.

In order to compute the radial displacement ΔR, one needs to know the conversion factor from radial to pulsational velocity p. Previous studies have shown that a value of 1.36 must be used for CORAVEL, when a Gaussian is fitted to the cross-correlation function (Burki et al. 1982).

4.1. Radii and distances

Having in hand all the necessary material, it is now straightforward to apply the Baade-Wesselink method exposed in the preceding subsection. We show two examples illustrating the method in Fig. 8 and Fig. 9. The radii and absolute magnitudes are given in Table 2. We now give some details for stars that deserve more attention.

BB Gem. Harris (1985) suggested that it could be a Pop II star, however Loomis et al. (1988) consider it as a Pop I. Other arguments in favor of the Pop. II hypothesis are its low radius (see Table 2) and its low galactic rotation velocity (F. Pont, private communication). We will thus consider BB Gem as a Pop. II Cepheid.

DX Gem. This star is a suspected binary (Bersier et al. 1994b). One should recall that a companion will modify the radius de-

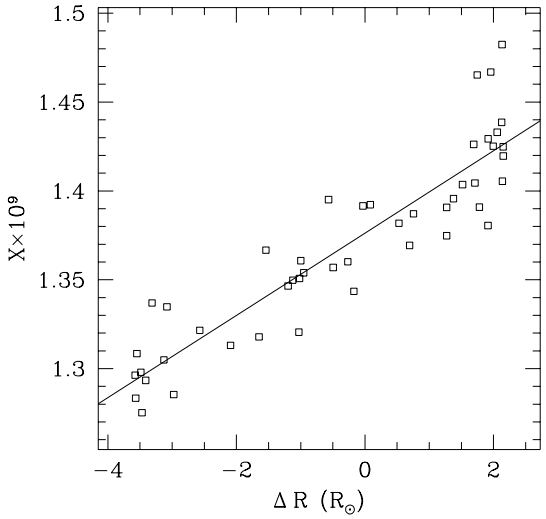

Fig. 8. The quantity X plotted versus ΔR for U Sgr, a classical Cepheid with a well determined radius.

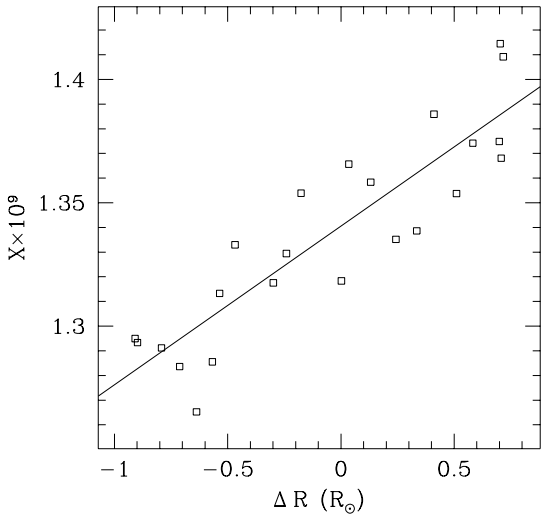

Fig. 9. The quantity X plotted versus ΔR for SZ Tau, an *s-Cepheid.*

rived by the Baade-Wesselink method. Balona (1977) showed that a hot companion decreases the radius, whereas a cool (K0) companion gives a larger radius. The small radius that we found could be the sign of the presence of a hot companion.

V473 Lyr. This is a very peculiar star whose pulsation amplitude varies by a factor $\sim$ 15 (Burki et al. 1986, Burki 1994). We have only a low number of photometric measurements (16) and the uncertainty is large, however a radius of 25 $R_\odot$ is another indication that this star could be pulsating in the second overtone (Burki et al 1986., Simon 1985).

V465 Mon. This is also a probable binary Cepheid (Bersier et al. 1994b), so the same remark as for DX Gem applies. The companion should also be hotter than the Cepheid.

Table 2. The radii, distances and absolute magnitudes for 20 Cepheids. The colour excesses are recalled to allow easier comparison with other works. The uncertainties on the radii and distances come from the statistical errors on the coefficients A and B (see Eq. 7)

Star	Class	$\log P$	Radius ($R_\odot$)	Distance	M_V	E(B-V)
V473 Lyr	2^{nd} ov.	0.1734	25.0 ± 19.0	468 ± 364	-2.52	0.109
SW Tau	II	0.1996	12.6 ± 2.8	1101 ± 258	-1.10	0.201
EU Tau	s	0.3227	30.0 ± 9.0	1267 ± 407	-3.03	0.195
BB Gem	II	0.3633	14.8 ± 5.8	2114 ± 840	-1.45	0.420
DT Cyg	s	0.3978	44.6 ± 17.7	780 ± 326	-3.73	0.015
BE Mon	C	0.4322	26.2 ± 4.1	1912 ± 335	-2.52	0.546
V465 Mon	s	0.4335	28.6 ± 14.9	3212 ± 1717	-3.01	0.269
DX Gem	s	0.4965	22.1 ± 7.9	2057 ± 766	-2.37	0.497
SZ Tau	s	0.4982	20.8 ± 2.3	342 ± 45	-2.08	0.300
ST Tau	C	0.6058	39.4 ± 4.8	1281 ± 181	-3.36	0.343
V508 Mon	C	0.6163	33.2 ± 8.8	3189 ± 890	-3.07	0.336
T Vul	C	0.6469	38.5 ± 4.2	585 ± 75	-3.22	0.052
U Sgr	C	0.8290	59.5 ± 4.1	793 ± 71	-4.10	0.426
W Sgr	C	0.8805	56.0 ± 2.9	444 ± 33	-3.83	0.088
V636 Cas	s	0.9230	82.6 ± 32.3	1071 ± 440	-4.70	0.562
S Nor	C	0.9892	81.6 ± 5.8	1167 ± 107	-4.48	0.186
ζ Gem	s	1.0065	89.5 ± 13.3	498 ± 84	-4.59	0.000
V340 Nor	s	1.0526	96.4 ± 14.0	2622 ± 434	-4.79	0.347
X Cyg	C	1.2145	97.6 ± 16.1	1069 ± 189	-4.45	0.242
SV Vul	C	1.6532	155 ± 12	1584 ± 148	-5.49	0.581

V440 Per. This Cepheid has a very low amplitude ($\Delta V \simeq 0.09$ mag). This could explain why we obtain a negative radius! This is caused by the fact that the dispersion of the points in the X vs ΔR diagram (as in Fig. 8) is larger than the total radius variation, giving an almost vertical fitted line. Thus it is not very surprising to have an extremely large negative radius.

W Sgr. This star is a well-known binary (Babel et al. 1989). However our Baade-Wesselink solution is in very good agreement with other Period-Radius relations (Gieren et al. 1989, Laney & Stobie 1995), indicating that the companion has almost no influence on the derived radius.

SW Tau. This is a Pop. II Cepheid (Harris 1985). We find a small radius which gives an a fortiori confirmation of the Pop. II nature of BB Gem.

SZ Tau. The small radius that we derived could be indicative of the presence of a blue companion, though a bluer limit at a spectral type A1 has been given by Evans (1992) on the basis of an IUE spectrum.

SV Vul. We find quite a small radius for SV Vul. One way of having a larger radius is to change the colour excess from 0.581 (the value we used) to $\sim$ 0.43 (Dean et al. 1978). Such a large change increases the radius up to 172 $R_\odot$, which is still a little bit

too low. Another solution is binarity since a marginal variation of the center-of-mass velocity has been detected (Bersier et al. 1994b).

A point that is exemplified by V440 Per is that the errors in R and M_V are larger for *s* Cepheids than for classical Cepheids. This is most certainly caused by the dispersion in the X values, when it becomes a non-negligible fraction of the total amplitude in X. Small amplitude (*s*) Cepheids are of course more sensitive to this effect.

From the values given in Table 2, it is tempting to try to derive Period-Radius and Period-Luminosity relations. Before doing this, several stars have to be excluded: SW Tau and BB Gem are Pop. II stars; V473 Lyr is most likely pulsating in the second overtone. Then we used the classification proposed by Bersier & Burki (1996) to separate classical and *s*-Cepheids. After that, we could derive PR and PL relations for each class; they are given below with their associated uncertainties. For 8 C-Cepheids (without SV Vul) we have

$$\log R = 0.769\,(\pm 0.063)\ \log P + 1.096\,(\pm 0.051) \quad (8)$$

with a dispersion $\sigma = 0.038$. For *s*-Cepheids, the relation is

$$\log R = 0.813\,(\pm 0.185)\ \log P + 1.116\,(\pm 0.129) \quad (9)$$

with a dispersion $\sigma = 0.135$. The Period-Luminosity relation for C-Cepheids (8 stars) is

$$M_{\rm V} = -2.62\,(\pm 0.39)\ \log P - 1.59\,(\pm 0.32) \quad (10)$$

with a dispersion $\sigma = 0.240$. The Cepheid SV Vul has not been taken into account because its uncertain colour excess and possible binarity make the radius uncertain. Fig. 10 illustrates the PR relation. An encouraging fact is the small dispersion (0.038) obtained for eight classical Cepheids, this is comparable to what has been obtained with much larger samples (Gieren et al. 1989, Laney & Stobie 1995). For comparison, Fig. 10 shows two other PR relations obtained with the surface brightness technique (Gieren et al. 1989, Laney & Stobie 1995). Our relation is not significantly different from theirs, though we predict slightly larger radii than Laney & Stobie, at all radii.

The Period-Luminosity relation is shown on Fig. 11. Here again the mean dispersion is comparable to recent results (e.g. Gieren et al. 1993). In this case, the coefficients are different from those of recent PL relations (e.g. Gieren et al. 1993). However, the low number of stars can explain why we have different results; the fit is very sensitive to the inclusion or exclusion of any given star. The mean dispersion is also larger than for the PR relation, this is certainly caused by the effect of the extinction, the magnitudes directly depend on $A_{\rm V}$ whereas the radius is only slightly affected by the absorption and not in a simple way.

About *s*-Cepheids, the errors in the coefficients of the PR and PL relations are much larger than for classical Cepheids. This is due to the larger individual errors on the radii and luminosities for *s*-Cepheids. We clearly need to increase the size of our sample in order to have a better determination of these coefficients.

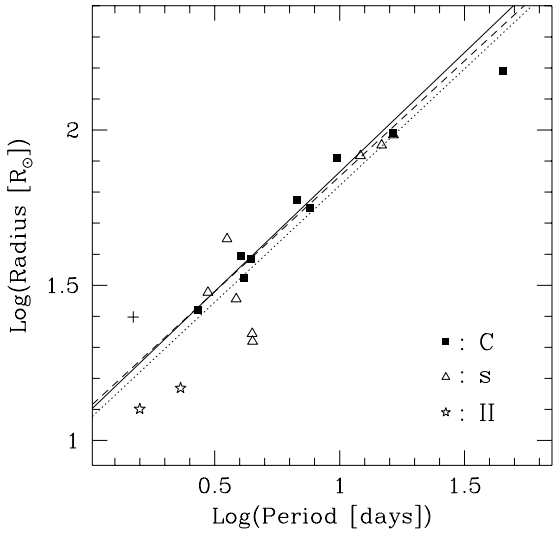

Fig. 10. The solid line is the Period-Radius relation for eight classical Cepheids, without SV Vul. Filled squares are for classical Cepheids, open triangles are for first overtone pulsators and the cross is for V473 Lyr. The dashed line shows the PR relation of Gieren et al. (1989)

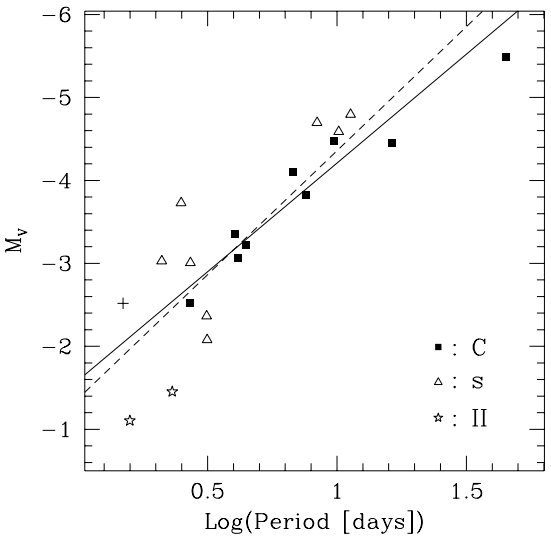

Fig. 11. The solid line is the Period-Luminosity relation for eight classical Cepheids, without SV Vul. Filled squares are for classical Cepheids, open triangles are for first overtone pulsators and the cross is for V473 Lyr. The dashed line is the PL relation of Gieren et al. (1993)

It is now clear, from the results of the MACHO and EROS microlensing surveys, that *s*-Cepheids are first overtone pulsators (Alcock et al. 1995, Beaulieu et al. 1995). From the period ratio as a function of (fundamental) period given in Alcock et al., we can compute the fundamental period, knowing the first overtone period. This allows to plot the *s*-Cepheids at the place they would be if they were fundamental mode pulsators.

One can then derive PR and PL relations as if one had only fundamental mode Cepheids. The relations are

$$\log R = 0.782\,(\pm 0.102)\ \log P + 1.050\,(\pm 0.085) \qquad (11)$$

with $\sigma = 0.100$ and

$$M_V = -2.76\,(\pm 0.46)\ \log P - 1.41\,(\pm 0.38). \qquad (12)$$

with $\sigma = 0.45$. The PR relation is even in better agreement with the one of Laney & Stobie (1995), showing the convergence obtained when microturbulence and gravity effects are taken into account.

We will refrain from commenting further these relations since they have been obtained with small samples, perhaps contaminated by binaries. The PR and PL relations are not definitive. We deduced them in order to check our results by comparing them with other published relations. The uncertainties on the coefficients of Eqs. 9 and 10 are large and we have to enlarge our sample of Cepheids to reduce these uncertainties.

5. Summary and conclusions

The first result of this paper is a new temperature scale for Cepheids based on atmosphere models. This scale is slightly warmer than previous ones. The cause is that the microturbulent velocity is larger than 2 km s^{-1} in most Cepheids, a value that has been commonly used in the past for such calibrations. In Fig. 4, there is a very good agreement between our temperature scale and Pel's one (1978). This is not surprising since he used a value of 4 km s^{-1} for the microturbulent velocity. This value, though constant, is closer to observed microturbulent velocity than 2 km s^{-1}.

Since temperature and reddening effects are intricate, one can always invoke a systematic error in the reddening scale. In our case, this seems very unlikely because the comparisons made in Bersier (1996) showed that our reddenings are slightly *lower*, if different, than those from other authors. This means that the higher temperatures found in this study are not a consequence of a too large reddening correction.

In the procedure that has been adopted for deriving temperatures from the observed colours, we made the implicit assumption that there is a one-to-one relation between the observed microturbulent velocity and the synthetic one. Should we not have tried to calibrate the synthetic ξ_t against the observed one? The results that have been found give us confidence in the correctness of this temperature scale: the synthetic gravity has a clear physical sense, our temperatures compare well with other scales. Thus, we can consider that this one-to-one relation really exists. If it was not the case, a relation between model microturbulence and observed one would not qualitatively alter the results. More particularly, the clear link between synthetic and effective gravity would still be present since such a relation would only stretch or compress the vertical scale of the gravity in Figs. 5, 6 and 7.

It is impossible to calibrate the gravity because there is no correlation between synthetic and spectroscopic values. This is a long-standing disagreement that certainly requires a deeper understanding of the atmospheres of cool, extended stars (see e.g. Luck & Wepfer, 1995). However, the appearance of the gravity curve obtained from the observed colours and the models shows that the gravity derived in this way for Cepheids is deeply connected to the effective gravity, that contains a dynamical component. This could be helpful when trying to find the cause of the difference between spectroscopic and synthetic gravity that is seen in non-variable supergiants. High resolution Cepheid spectra at different phases would allow to derive a curve showing the variation of the spectroscopic gravity. The comparison of the curve so-obtained with the effective gravity should be very interesting.

The use of the cross-correlation function to measure radial velocities and microturbulent velocities means that all the physics of the atmosphere is contained in one single "mean" line. This is a limitation of our approach since it is now clear that, for instance, the projection factor, p, varies with the phase (Albrow & Cottrell 1996, Sabbey et al. 1995). Another cause of systematic errors could be the presence of a velocity gradient, particularly near maximum infall velocity. Such a velocity gradient had already been suspected of being the cause of the observed difference between the synthetic and the observed gravity near minimum radius.

The main advantages of our version of the Baade-Wesselink method are

i) it is an exact solution, not a linearized version
ii) the temperature and bolometric correction are explicitly determined, *taking into account the gravity and microturbulence variations*
iii) there is no further uncertainty introduced by a colour-temperature relation
iv) The radius and distance are simultaneously determined
v) *All* photometric measurements are used simultaneously to constrain the solution (though this is the case in most modern Baade-Wesselink realizations)

The method works very well for classical Cepheids but the errors are larger for *s*-Cepheids; this causes a higher dispersion in the PR and PL relations. The strongest conclusion is the fact that a Baade-Wesselink analysis based on visible photometry can be as accurate as in the infra-red, *provided that microturbulence variations are taken into account*.

The Period-Radius and Period-Luminosity relations that we obtained are slightly different from other published results. However, the low number of stars can explain these differences because the presence or absence of one star can noticeably change the slopes and zero points. Our aim in this paper was to test the method and to compare our preliminary results with published relations. A more complete study awaits a larger sample of Cepheids with the necessary data.

Acknowledgements. We thank Dr. R. E. Luck for discussions and advices. This work has been partly supported by the Swiss National Science Foundation. This research has made use of the Simbad database, operated at CDS, Strasbourg, France

References

Albrow M.D., Cottrell P.L., 1996, MNRAS 278, 337
Alcock C., Allsman, R.A., Axelrod T.S. et al. 1995, AJ 109, 1654
Babel J., Burki G., Mayor M., Waelkens C., Chmielewski Y., 1989, A&A 216, 125
Balona L.A., 1977, MNRAS 178, 231
Baranne A., Mayor M., Poncet J. L., 1979, Vistas Astron., 23, 279
Barnes T.G., Evans D.S., 1976, MNRAS 174, 489
Beaulieu J.-P., Grison P., Tobin W. et al. 1995, A&A 303, 137
Bersier D., Burki G., Burnet M., 1994a, A&AS 108, 9 (Paper I)
Bersier D., Burki G., Mayor M., Duquennoy A., 1994b, A&AS 108, 25 (Paper II)
Bersier D., 1996, A&A , 308, 514
Bersier D., Burki G., 1996, A&A , 306, 417 (Paper III)
Böhm-Vitense E., 1972, A&A 17, 335
Burki G., Mayor M., Benz W., 1982, A&A 109, 258
Burki G., Meylan G., 1986, A&A 156, 131
Burki G., Schmidt E.G., Arellano Ferro A., Fernie J.D., Sasselov D., Simon N.R., Percy J.R., Szabados L., 1986, A&A 168, 139
Burki G., 1994, In: C. Sterken, M. de Groot (eds), The Impact of Long Term Monitoring on Variable Star Research, Kluwer Academic Publishers, Dordrecht, The Netherlands, p. 247
Castelli F. 1994, private communication
Castelli F. 1996, proceedings of the 5th Vienna Workshop, Model atmospheres and spectrum synthesis. ASP Conf Series, in press
Dean J.F., Warren P.R., Cousins A.W.J., 1978, MNRAS 183, 569
Evans N.R., 1992, ApJ 384, 220
Flower P.J., 1977, A&A 54, 31
Fokin A., Gillet D., Breitfellner M., 1996, A&A 307, 503
Gieren W.P., 1989, A&A 225, 381
Gieren W.P.,, Barnes T.G., Moffet T.J., 1989, ApJ 342, 467
Gieren W.P.,, Barnes T.G., Moffet T.J., 1993, ApJ 418, 135
Golay M., 1980, Vistas Astron., 24, 141
Harris H.C., 1985, AJ 90, 756
Johnson H.L., 1966, ARA&A 4, 193
Karp A.H., 1975, ApJ 200, 354
Kobi D., North P., 1990 A&AS 85, 999
Künzli M., North P., Nicolet B., Kurucz R.L., 1997, A&A , in press
Kurucz R.L., 1991, In: A.G. Davis Philip, A.R. Upgren and K.A. Janes (eds) Precision Photometry. L. Davis Press, p. 27
Kurucz R.L., 1992, In: B. Barbuy, A. Renzini (eds) Proc. IAU Symp. 149, The stellar populations of galaxies. Kluwer, p. 225
Kurucz R.L., 1993, CD-ROM 13 (ATLAS9 stellar atmosphere program and 2 km s^{-1} grid)
Kurucz R.L., 1994, CD-ROM 19 (Solar abundance atmosphere models for 0,1,2,4,8 km s^{-1})
Kurucz R.L., 1996, in preparation, CD-ROMs 24 and 25 (will replace CD-ROMs 13 and 19 respectively)
Lambert D.L., Ries L.M., 1981, ApJ 248, 228
Laney C.D., Stobie R.S., 1995, MNRAS 274, 337
Lester J.B., Gray R.O., Kurucz R.L., 1986, ApJS 61, 509
Loomis C., Schmidt E.G., Simon N.R., 1988, MNRAS 235, 1059
Luck R.E., 1991, ApJS 75, 579
Luck R.E., Wepfer G.G., 1995, AJ 110, 2425
McWilliam A., 1991, AJ 101, 1065
North P., Nicolet B., 1990, A&A 228, 78
Pel J.W., 1978, A&A 62, 75
Pel J.W., 1985, In: B. F. Madore (ed) Proc IAU Coll. 82, Cepheids: Theory and Observations. Cambridge University Press, Cambridge, p. 1
Rufener F., 1988, Catalogue of stars measured in the Geneva Photometric system (4th ed.), Observatoire de Genève, Switzerland
Rufener F., Nicolet B., 1988, A&A 206, 357
Sabbey C.N., Sasselov D.D., Fieldus M.S., Lester J.B., Venn K.A., Butler R.P., 1995, ApJ 446, 250
Simon N.R., 1985, In: B. F. Madore (ed) Proc IAU Coll. 82, Cepheids: Theory and Observations. Cambridge University Press, Cambridge, p. 93
Simon N.R., Kanbur S.M., Mihalas D., 1994, ApJ 414, 310
Tripicco M.J., Bell R.A., 1991, AJ 102, 744

This article was processed by the author using Springer-Verlag LaTeX A&A style file *L-AA* version 3.